J|A|C|S COMMUNICATIONS

Published on Web 09/18/2009

Cell-Directed Localization and Orientation of a Functional Foreign Transmembrane Protein within a Silica Nanostructure

Eric C. Carnes,[†] Jason C. Harper,[†,§] Carlee E. Ashley,[†] DeAnna M. Lopez,[†] Lina M. Brinker,[†] Juewen Liu,[†] Seema Singh,[†] Susan M. Brozik,[†,§] and C. Jeffrey Brinker*[,†,‡,§]

Department of Chemical and Nuclear Engineering and Department of Molecular Genetics and Microbiology, University of New Mexico, Albuquerque, New Mexico 87131, and Sandia National Laboratories, Albuquerque, New Mexico 87106

Received July 20, 2009; E-mail: cjbrink@sandia.gov

The development of new material behaviors based on incorporation of stable and functional biomolecules has attracted considerable interest because of potential applications in biotechnology, biocatalysis, drug delivery, bioelectronic devices, and biological sensing.[1] Recently, the use of sol−gel technology to immobilize functional soluble proteins in inorganic materials has been widely reported. This success is largely due to advances in sol−gel processing that reduce the exposure of biological components to alcohol solvents, toxic byproducts, and the highly acidic or basic conditions of hydrolysis.[2] Similar advances in the development of biocompatible sol−gel processes have also permitted the encapsulation of viable cells.[3] The extension of these biologically compatible sol−gel processing techniques to the encapsulation of more sensitive membrane-bound proteins in sol−gel matrices remains a significant challenge.[4] The relatively few successful reports of membrane protein encapsulation mostly utilize the photoactive protein-retinal complex bacteriorhodopsin (bR). This prior work demonstrated that bR retained native photoinduced proton pumping functionality but that this function was rather inconsequential, as the proteins were randomly oriented and therefore could not yield useful ion gradients.[5] Specific orientation of bR in sol−gel matrices was recently achieved using silica-entrapped bR-proteoliposomes (liposome-reconstituted bR) to produce proton gradients that facilitated ATP synthesis[6] and by intercalation of silica between oriented sheets of intact purple membrane lipid bilayers, which when integrated on an electrode produced measurable photocurrents.[7]

We recently reported that through the use of short-chain phospholipids to direct the formation of thin-film silica nanostructures during evaporation-induced self-assembly[8] (EISA), the introduction of cells profoundly alters the inorganic self-assembly pathway. Cells actively organize around themselves an ordered, multilayered lipid membrane that interfaces coherently with a 3D lipid-templated silica nanostructure. This bio/nano interface is unique in that it withstands drying (even evacuation), maintaining cell viability for days to years without external buffer, yet remains accessible to molecules, proteins/antibodies, plasmids, etc. introduced into the 3D silica host.[9] Herein we report an extension of this cell-directed assembly approach in which bR is oriented within a multilayered lipid membrane localized at the interface between *Saccharomyces cerevisiae* and the surrounding lipid-templated silica matrix. To the best of our knowledge, this is the first report detailing incorporation of both functional transmembrane bacterial proteins and viable cells in a sol−gel material. Importantly, the bR is observed to modulate pH gradients developed at the cell surface, demonstrating both orientation and retained functionality. Such a simple procedure for introducing functional exogenous membrane-bound proteins into immobilized cells may significantly impact fundamental studies of membrane protein function and cell−cell signaling.

The two methods used by us to introduce bR and yeast cells into a lipid-templated silica matrix are depicted in Figure 1A. In both methods, equal volumes of sol precursors and yeast cells, suspended in phosphate buffer, were mixed (see the Supporting Information). In one method, bR was added directly to the yeast solution along with short zwitterionic diacylphosphatidylcholines (diC_6 PC). Alternatively, bR was first incorporated into dimyristoylphosphatidylcholine (DMPC) liposomes (see the Supporting Information) and then added to the yeast solution with diC_6 PC. Following mixture of the respective yeast solutions with sol precursors, the solutions were immediately spin-coated onto glass substrates. Grazing-incidence small-angle X-ray scattering (GISAXS) and scanning electron microscopy (SEM) were used to characterize the cell−lipid−protein−silica matrix produced from each of the two methods shown in Figure 1A. Consistent with our previous studies,[8] films prepared using either method exhibited lamellar structures with a repeat distance (d_r) of ∼31 Å as a result of the cell-directed assembly process (Figure 1B). Also consistent with our previous reports, SEM imaging of samples prepared using either method showed *S. cerevisiae* encapsulated in a crack-free silica film with a coherent cell−matrix interface (Figure 1C).

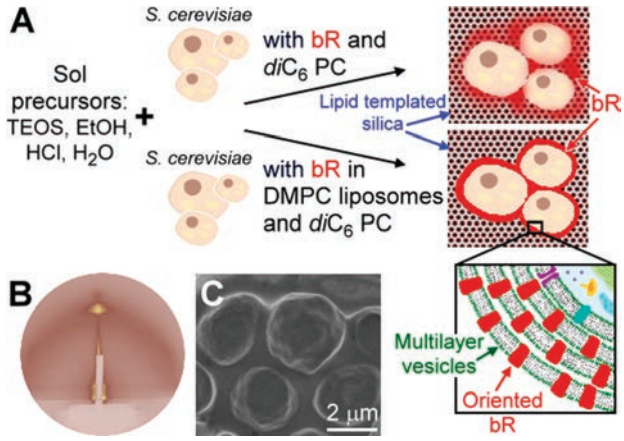

Figure 1. (A) Encapsulation of yeast and bacteriorhodopsin (bR) in mesostructured silica films by direct addition of bR or addition of bR incorporated into DMPC liposomes to the yeast/diC_6 PC lipid/sol precursor solution. bR added directly to diC_6 PC was localized in a disordered and diffuse fashion, while bR incorporated into DMPC liposomes and added to the diC_6 PC/yeast solution was preferentially localized near the yeast cell surface, forming conformal bR-containing multilayer vesicles. (B) GISAXS pattern of the lipid−silica matrix-encapsulated yeast−bR film, showing the lamellar structure. (C) SEM image of the lipid−silica matrix-encapsulated yeast−bR film.

[†] Department of Chemical and Nuclear Engineering, University of New Mexico.
[‡] Department of Molecular Genetics and Microbiology, University of New Mexico.
[§] Sandia National Laboratories.

Localization of the protein and various lipid components was monitored by fluorescent labeling and laser-scanning confocal fluorescence microscopy. Pronounced differences in lipid and protein localization near *S. cerevisiae* cells were observed when samples prepared by direct addition of bR or addition of bR-proteoliposomes to the yeast/*di*C_6 PC solution were compared. Figure 2A shows that upon addition of bR directly to the yeast/*di*C_6 PC solution, bR (red panel) was localized near *S. cerevisiae* cells in a diffuse manner that corresponded closely to the region of *di*C_6 PC localization (green panel). Localization of *di*C_6 PC near yeast cells is consistent with our previous studies showing the formation of a lipid-rich region that interfaces cells with the surrounding nanostructured silica host. Figure 2B shows that addition of bR-proteoliposomes to the yeast/*di*C_6 PC solution resulted in a more conformal localization of bR (red panel) near *S. cerevisiae* cells. The thickness of the protein layer suggests that multiple fusion steps occurred during cell-directed assembly, forming yeast-supported multilayers containing bR. Figures 2B and 3A show that longer-chain lipids introduced as liposomes with (Figure 2B) or without (Figure 3A) bR preferentially localize at yeast cell surfaces during cell-directed assembly. In Figure 2B, preferential localization of NBD-labeled longer-chain palmitoyloleoyl phosphatidylcholine (POPC) (introduced as 1% of the total liposome lipid, green panel) is clearly shown by the 4−5 cells in which the confocal slice includes the top portion of the cells (peripheral cells). On the basis of additional cell-directed assembly experiments performed with labeled liposomes and labeled *di*C_6 PC (e.g., Figure 3A), we propose that bR introduced in proteoliposomes is colocalized with both the longer-chain liposomal lipids and the shorter-chain lipids in close proximity to the cell surface but that the bR and liposomal lipids have higher priority for and are more conformal with the cell surface.

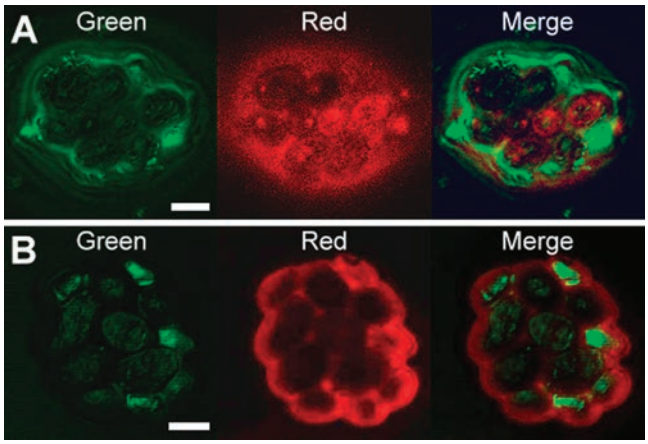

Figure 2. Confocal fluorescence images of Alexa Fluor 594-labeled bR (red emission) localized near yeast cells in the surrounding lipid−silica matrix. (A) bR added with *di*C_6 PC only (1% NBD-labeled *di*C_6 PC, green emission) to yeast. (B) bR incorporated into DMPC liposomes (1% NBD-labeled POPC, green emission) added with *di*C_6 PC to yeast. Scale bars = 3 μm.

The importance of evaporation-induced cell-directed assembly in forming yeast-supported bR multilayers is evidenced by the lack of spontaneous liposome fusion or lipid association around yeast cells in buffered solutions. In these control experiments, yeast and POPC liposomes (6% Texas Red-labeled DHPE) were mixed with and without *di*C_6 PC in buffered solutions prepared at various pH values: pH 7 (pH of the initial bR-proteoliposome/yeast/*di*C_6 PC solution prior to adding sol precursors), pH 2 (pH of the silica precursor solution), and pH 5 (pH obtained near the lipid/silica-encapsulated cells following cell-directed assembly). In each case, neither liposome fusion nor lipid association with yeast cells was observed, showing that neither electrostatic effects over the pH range studied nor the presence of *di*C_6 PC induce liposome fusion with the yeast cells in solution. POPC liposome fusion and multilayer formation around yeast cells was observed, however, when liposomes were added to a yeast/*di*C_6 PC/sol precursor solution and spin-coated onto a cover glass. As shown in Figure 3A, during evaporation-induced cell-directed assembly, both the longer-chain liposome lipid (6% Texas Red-labeled DHPE, red panel) and shorter-chain *di*C_6 PC lipid (1% NBD-labeled, green panel) are localized at the cell surface, but the longer-chain lipid is more conformal and has greater priority for the cell surface (merged image). Additionally, it is important to note that viable cells play an active role in the formation of yeast-supported bR multilayers. In control experiments using neutrally charged latex beads as cell surrogates, neither localization of liposome lipid (Figure 3B) nor bR (Figure 3C) occurred upon evaporation.

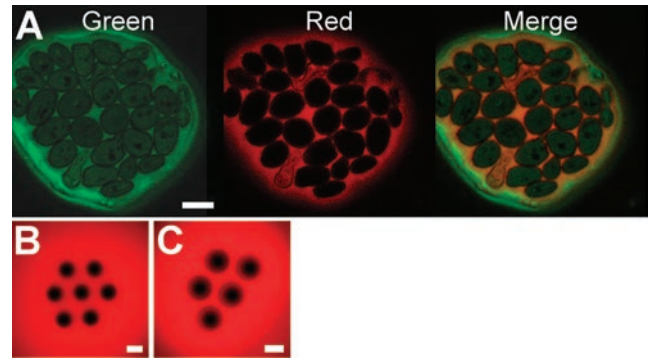

Figure 3. (A) Confocal fluorescence image showing liposome fusion and multilayer formation around yeast cells during cell-directed assembly. POPC liposomes (6% Texas Red-labeled DHPE, red emission) were added to a yeast/*di*C_6 PC (1% NBD-labeled, green emission)/sol precursor solution. (B−C) Confocal projections of cell surrogates (neutrally charged latex beads) added to the *di*C_6 PC/sol precursor solution, showing that (B) POPC liposomes (2.5% Texas Red-labeled DHPE) and (C) Alexa Fluor 594-labeled bR in DMPC liposomes are not localized. Scale bars = 3 μm.

The ability to generate a photoinduced proton gradient in the lipid−protein−cell−silica matrix was investigated using the membrane-impermeant, pH-sensitive fluorescent dye Oregon Green. As shown in Figure 4A, the intensity of fluorescent emission decreased as the pH was lowered from ~6 to 3, with total quenching of fluorescence at highly acidic pH (≤2). The pH gradient resulting from exposure of the films to green light[10] is shown using the confocal *z*-axis projections in Figure 4B−D. As we have previously shown, encapsulated cells form a pH gradient from pH ~3 in the acidic silanol-terminated silica matrix to pH 5.5 at the encapsulated cell surface, spanning a distance of several micrometers. Figure 4B shows that a film prepared from addition of DMPC liposomes (without bR) to the yeast/*di*C_6 PC lipid solution and exposure of the film to green light (see the Supporting Information) yielded similar pH gradients, with pH near 5 at the cell surfaces decreasing to pH ~3 over a few micrometers. Photoinduced proton pumping was observed in samples prepared from direct addition of bR to the yeast/*di*C_6 PC solution (Figure 4C), which shows a slight decrease in pH to 4.5 at the cell surface, as evidenced by the reduced intensity of the Oregon Green dye relative to Figure 4B. This slight decrease in pH is indicative of nonfunctional and/or randomly oriented bR, as functionality requires a lipid bilayer that can accommodate the hydrophobic domains of the transmembrane protein.

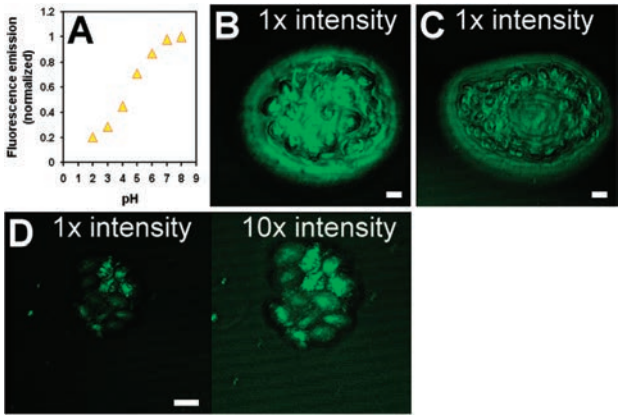

Figure 4. (A) pH dependence of the fluorescence emission of the pH-sensitive probe Oregon Green. (B−D) Confocal projections comparing the development of pH gradients using Oregon Green in mesostructured silica-encapsulated yeast with (B) DMPC liposomes without bR but with *di*C_6 PC, (C) bR added with *di*C_6 PC only, and (D) bR added in DMPC liposomes with *di*C_6 PC. Decreasing fluorescence intensity corresponds to decreasing pH. Scale bars = 3 μm.

Dramatic changes in the pH gradient were observed for samples prepared by addition of bR-proteoliposomes to the yeast/*di*C_6 PC solution. As shown in Figure 4D, the original several-micrometer region of higher pH surrounding the encapsulated cells is no longer present. Increasing the fluorescence intensity by 10-fold (Figure 4D) shows that the region surrounding the cells containing bR is now similar in pH to the surrounding silica matrix, ~pH 3−4, consistent with proton pumping toward the cell. Unfortunately, because of the strongly overlapping spectral windows of Oregon Green emission and bR absorption and activation (Figures S1 and S2) attempts to image the initial pH gradient were unsuccessful—confocal imaging unavoidably stimulates proton pumping, eradicating the initial pH gradient. However, it is clear that the Oregon Green dye penetrates the multilayer vesicle region, retaining its capability to probe pH near the yeast cells, and does not photobleach significantly over the course of these experiments, as shown by the bright-green emission when bR was absent (Figure 4B). [Further addition of exogenous buffer (pH 7.0) caused immediate uniform green emission throughout the matrix.] The decrease in pH by ~2 units over the typically 15 min required to locate cells and obtain the confocal projection was similar to that previously reported for bR reconstituted in porous silica microsphere-supported bilayers.[11] In that study, after a 60 min exposure of the 10 μm diameter microspheres to a UV-filtered xenon lamp, a pH change of 1.5 units was observed and attributed to bR orientation on the microsphere surface driven by fusion of unidirectionally aligned bR proteoliposomes with the microsphere.[11] For our system, the comparatively smaller volume of the lipid−protein-encapsulated cells (>37× smaller for ~3 μm diameter yeast cells than for microspheres) and higher intensity of the laser light are consistent with a moderately greater pH change over a shorter time period.

These results show that bR retain their native functionality and adopt a preferred orientation with respect to the yeast cellular surface when introduced in proteoliposomes with *di*C_6 PC. It has been shown that bR inserts unidirectionally into preformed liposomes under conditions of detergent saturation.[12] *di*C_6 PC may act as a detergent that upon EISA and cell-directed assembly reaches saturated concentration near the cells. This causes destabilization of the colocalized bR-proteoliposomes, facilitating fusion of liposomes with other liposomes and the unidirectional orientation of bR.[12] This thesis is supported by the lack of liposome fusion or bR localization near neutrally charged latex beads (Figure 3B,C) which we have shown do not localize *di*C_6 PC under evaporation-induced cell-directed assembly.[8] The inside-out orientation of bR reported in this work is identical to the bR orientation reported for bR-proteoliposomes formed in the presence of saturating detergent. Additionally, the proposed mechanism that proteins always insert through the hydrophobic domain of the membrane with the more hydrophobic protein moiety[13] is followed by this system, where the more hydrophobic NH_2-terminal region of bR penetrates the yeast-supported multilayers, yielding an inside-out orientation.

In summary, we have shown a simple method for interfacing and orienting functional exogenous membrane-bound proteins with cells. We expect this method to be general and adaptable to other membrane-bound proteins. It may prove useful in fundamental studies of membrane protein function and in imparting non-native characteristics to arbitrary cells.

Acknowledgment. This work was funded by the Air Force Office of Science and Research (AFOSR), the DOE Office of Science, Office of Basic Energy Sciences, the Defense Threat Reduction Agency (DTRA) CB Basic Research Program, and Sandia's LDRD Program. We thank Constantine Khripin for measuring the pH dependence of Oregon Green fluorescence emission. Sandia is a multiprogram laboratory operated by Sandia Corporation, a Lockheed Martin Company, for the United States Department of Energy under Contract DE-AC04-94AL85000.

Supporting Information Available: Methods. This material is available free of charge via the Internet at http://pubs.acs.org.

References

(1) (a) Avnir, D.; Coradin, T.; Lev, O.; Livage, J. *J. Mater. Chem.* **2006**, *16*, 1013. (b) Hartmann, M. *Chem. Mater.* **2005**, *17*, 4577. (c) Ispas, C.; Sokolov, I.; Andreescu, S. *Anal. Bioanal. Chem.* **2009**, *393*, 543. (d) Lee, M.-Y.; Park, C. B.; Dordick, J. S.; Clark, D. S. *Proc. Natl. Acad. Sci. U.S.A.* **2005**, *102*, 983.
(2) (a) Braun, S.; Rappoport, S.; Zusman, R.; Avnir, D.; Ottolenghi, M. *Mater. Lett.* **1990**, *10*, 1. (b) Ellerby, L. M.; Nishida, C. R.; Nishida, F.; Yamanaka, S.; Dunn, B.; Valentine, J. S.; Zink, J. I. *Science* **1992**, *255*, 1113. (c) Yi, Y.; Neufeld, R.; Kermasha, S. *J. Sol-Gel Sci. Technol.* **2007**, *43*, 161.
(3) (a) Nassif, N.; Bouvet, O.; Rager, M. N.; Roux, C.; Coradin, T.; Livage, J. *Nat. Mater.* **2002**, *1*, 42. (b) Carturan, G.; Dal Toso, R.; Boninsegna, S.; Dal Monte, R. *J. Mater. Chem.* **2004**, *14*, 2087. (c) Amoura, M.; Nassif, N.; Roux, C.; Livage, J.; Coradin, T. *Chem. Commun.* **2007**, 4015.
(4) Brennan, J. D. *Acc. Chem. Res.* **2007**, *40*, 827.
(5) (a) Wu, S.; Ellerby, L. M.; Cohan, J. S.; Dunn, B.; El-Sayed, M. A.; Valentine, J. S.; Zink, J. I. *Chem. Mater.* **1993**, *5*, 115. (b) Weetall, H. H.; Roberston, B.; Cullin, D.; Brown, J.; Walch, M. *Biochim. Biophys. Acta* **1993**, *1142*, 211. (c) Weetall, H. H. *Biosens. Bioelectron.* **1996**, *11*, 327. (d) Shamansky, L. M.; Luong, K. M.; Han, D. H.; Chronister, E. L. *Biosens. Bioelectron.* **2002**, *17*, 227.
(6) Luo, T. J. M.; Soong, R.; Lan, E.; Dunn, B.; Montemango, C. *Nat. Mater.* **2005**, *4*, 220.
(7) Bromley, K. M.; Patil, A. J.; Seddon, A. M.; Booth, P.; Mann, S. *Adv. Mater.* **2007**, *19*, 2433.
(8) Baca, H. K.; Ashley, C.; Carnes, E.; Lopez, D.; Flemming, J.; Dunphy, D.; Singh, S.; Chen, Z.; Liu, N. G.; Fan, H. Y.; Lopez, G. P.; Brozik, S. M.; Werner-Washburne, M.; Brinker, C. J. *Science* **2006**, *313*, 337.
(9) Baca, H. K.; Carnes, E.; Singh, S.; Ashley, C.; Lopez, D.; Brinker, C. J. *Acc. Chem. Res.* **2007**, *40*, 836.
(10) (a) Birge, R. R. *Biochim. Biophys. Acta* **1990**, *1016*, 293. (b) Saaem, I.; Tian, J. *Adv. Mater.* **2007**, *19*, 4268.
(11) Davis, R. W.; Flores, A.; Barrick, T. A.; Cox, J. M.; Brozik, S. M.; Lopez, G. P.; Brozik, J. A. *Langmuir* **2007**, *23*, 3864.
(12) Rigaud, J.-L.; Paternostre, M.-T.; Bluzat, A. *Biochemistry* **1988**, *27*, 2677.
(13) Eytan, G. D. *Biochim. Biophys. Acta* **1982**, *694*, 185.

JA906055M